Nanorod-like α-Bi2O3 nanoparticles: a highly active photocatalyst synthesized by using g-C3N4 as a template

Journal:	*RSC Advances*
Manuscript ID:	RA-COM-08-2014-008541.R2
Article Type:	Communication
Date Submitted by the Author:	06-Oct-2014
Complete List of Authors:	Jiang, Haiying; National Institute for Materials Science, Research Unit for Enviromental Remediation Materials; Renmin University of China, Department of Chemistry Liu, Guigao; National Insititute for Materials Science, Research Unit for Enviromental Remediation Materials Science Li, Peng; National Insititute for Materials Science, Environmental Remediation Materials Unit Hao, Dong; National Insititute for Materials Science, Environmental Remediation Materials Unit Meng, Xianguang; National Insititute for Materials Science, Environmental Remediation Materials Unit Wang, Tao; Natioanal Insititute for Materials Science, Environmental Remediation Materials Unit Lin, Jun; Renmin University of China, Department of Chemistry Ye, Jinhua; National Insititute for Materials Science, Environmental Remediation Materials Unit

Cite this: DOI: 10.1039/c0xx00000x

www.rsc.org/xxxxxx

ARTICLE TYPE

Nanorod-like α-Bi_2O_3 nanoparticles: a highly active photocatalyst synthesized by using g-C_3N_4 as a template

Hai-Ying Jiang [a, b], Guigao Liu [a], Peng Li [a], Dong Hao [a], Xianguang Meng [a], Tao Wang[a], Jun Lin [b, *], Jinhua Ye [a, *]

Received (in XXX, XXX) Xth XXXXXXXXX 20XX, Accepted Xth XXXXXXXXX 20XX

DOI: 10.1039/b000000x

The nanorod-like α-Bi_2O_3 nanoparticles have been synthesized from the microrod-like α-Bi_2O_3 by using g-C_3N_4 as a template. The photocatalytic activity of α-Bi_2O_3 is highly improved by nearly 800% in the oxidation of the gaseous IPA (isopropyl alcohol). The formation mechanism of the nanorod-like α-Bi_2O_3 nanoparticles was further studied, and demonstrated to be the CO_2 corrosion effects.

Semiconductor photocatalysis, as a new rising discipline with the primary focus on anatase TiO_2, has attracted an increasing attentions and interests in the past decades[1]. This is mainly because it can directly convert the solar energy into chemical energy with the excitation of the semiconductors[2]. However, the only UV light response of the traditional photocatalysts highly limits their practical applications. In order to realize the extensive utilization of the solar light, some narrow band gap semiconductors have been proposed to develop the visible-light-responsive photocatalytic materials[3-5]. α-Bi_2O_3 is such a semiconductor with visible light response (Eg = 2.8 eV). Besides that, it can be seen as a potential photocatalyst candidate also because of its other distinctive properties, such as deep valence band, environment friendship (non-toxic and low-radioactivity), and thermal stability[6-10]. Nevertheless, α-Bi_2O_3 shows very poor activity as a photocatalyst, as previously reported[4-6, 11, 12]. Generally, the poor activity is considered to be caused by the following two aspects: ⅰ) its conduction band is too low (+ 0.33 eV *vs.* NHE) to oxide the surface O_2 into $O_2^{\cdot -}$ (-0.33 eV *vs.* NHE), leading to a high recombination rate of the photogenerated electrons and holes; ⅱ) the grain size of α-Bi_2O_3 prepared by the ordinary methods is too large (dozens of micrometers), resulting in a very low surface area[5]. About the first point, there have been many strategies being developed to decrease the recombination rate of the photogenerated electrons and holes[4-6, 11, 12]. But researches about the second point were rarely reported[13, 14]. As we know, the grain size and surface area are very important factors which strongly affect the photocatalytic activities. Therefore, preparing α-Bi_2O_3 nanoparticles by a simple method is very helpful for α-Bi_2O_3 to become a promising photocatalyst in the future research.

g-C_3N_4 is a novel stable metal-free photocatalyst with the band gap of 2.7 eV, and consequently can absorb visible light ($\lambda < 460$ nm)[15]. However, its photocatalytic activity is limited by the high recombination of the photocarriers[16]. As reported, heterojunction construction is one of the methods to enhance its photocatalytic activity[16-18]. In this study, however, the g-C_3N_4 was just only used as a template to synthesize the nanorod-like α-Bi_2O_3 nanoparticles from the microrod-like α-Bi_2O_3, to enhance the photocatalytic activity of α-Bi_2O_3. This work is derived from an accidental discovery in the construction processes of the α-Bi_2O_3/g-C_3N_4 heterojunctions. The microrod-like α-Bi_2O_3 was fabricated by a typical method in the earlier reports[5, 6]. The g-C_3N_4 was synthesized by heating the melamine at 520°C for 4 hours in a half-open system[11]. The g-C_3N_4 induced nanorod-like α-Bi_2O_3 nanoparticles were prepared as follows[12, 13]: The g-C_3N_4 and microrod-like α-Bi_2O_3 with different weight fractions were thrown into 100 ml alcohol (95%), following with 3 hours' ultrasonication and 24 hours' stirring at room temperature. Before the last calcinations at 450°C for 3 hours and 6 hours in a half-open system, the products were dried at 100°C for 12 hours in advance. The prepared samples were named as Sn, and 10*n equals to the weight fraction percentage of g-C_3N_4 in the mixture of α-Bi_2O_3/g-C_3N_4. The microstructures, surface areas, crystal structures, optical properties of the samples were studied by the scanning electron microscope (SEM), X-ray diffraction (XRD) combining with ultraviolet-visible light diffuse reflectance accessory (UV-vis DRS) and Fourier transform-infrared (FT-IR) spectra. The photocatalytic activities of the α-Bi_2O_3 samples were performed by the oxidation of the gaseous IPA. Furthermore, the formation mechanism of the nanorod-like α-Bi_2O_3 nanoparticles from the microrod-like α-Bi_2O_3 was studied detailedly by the combination of TG-DTA and XRD.

The microstructure changes of the α-Bi_2O_3 samples induced by g-C_3N_4 were listed in Figure 1. After the treatments of the α-Bi_2O_3 samples with different weight fractions of g-C_3N_4 for 3 hours' calcination, there are some pores emerged on the surface of the α-Bi_2O_3 microrods. The amounts of the pores show an increasing trend with the increase of the g-C_3N_4 weight fractions used in the prepared processes. For the S5 and S7, expectedly, the pore-structures of the α-Bi_2O_3 samples were further destroyed into smaller particles when the calcination time were prolonged to 6 hours from 3 hours, ultimately, resulting in the formation of the nanostructure α-Bi_2O_3. Since the particle size of the α-Bi_2O_3 decreased, the surface areas of the samples were speculated to have a gradually increase, and proved in Table 1. From Figure 2, we can clearly see that the shapes of the nanostructure α-Bi_2O_3 look like some nanorods with hundreds of nanometres' length, so we call it as nanorod-like α-Bi_2O_3 nanoparticles.

According to the XRD spectra of the α-Bi_2O_3 samples in Figure 3, the crystal structures of all the samples with 6 hours' calcinations show good crystals in a single monoclinic phase, being in accordance with the JCPDS file (No.41-1449)[5]. Obviously, the intensities of the main peaks (120) have sharply decreased for the S5 – 6h and S7 - 6h, indicating the disappearances of the preferred orientations. This is most probably caused by the exhaustive microstructure changes of the α-Bi_2O_3 samples. Surprisingly, we can't found any diffraction peaks of g-C_3N_4 in the XRD spectra of all the samples. According to the FT-IR spectra (Figure S1), no any vibration peaks derived from g-C_3N_4 (820 cm^{-1}, 890 cm^{-1}, 1000-1900 cm^{-1}, 1965 cm^{-1}, 2054 cm^{-1}, 2141 cm^{-1}, and 2800-3700 cm^{-1}) was observed in all the α-Bi_2O_3 samples; this means that g-C_3N_4 resolves out during the heat treatment process at the high temperature. The optical properties of the pure α-Bi_2O_3 samples with different microstructures were characterized by the UV-vis DRS spectra (Figure S2), showing no obvious changes occurs. Detailedly, there are some inconspicuous gradual blue shifts with the decrease of the particle size, indicating an increase of the band gaps (inset in Figure S2). The change of the band gap between microrod-like α-Bi_2O_3 and nanorod-like α-Bi_2O_3 is observed about 0.1 eV.

The photocatalytic activity of the as-prepared α-Bi_2O_3 samples were appraised by the oxidation of gaseous IPA. The production of acetone, the one-hole oxidation product of IPA, was monitored as the unique index to judge the reaction activities. Figure 4 describes the acetone productions over the α-Bi_2O_3 samples with different microstructures, under the visible light irradiations (420 nm $\leq \lambda \leq$ 800 nm) for 8 hours. Different α-Bi_2O_3 samples show different photocatalytic activities, although all of them can oxidize the IPA to acetone under visible light irradiations. With the weight fraction increase of the g-C_3N_4 used in the prepared process, the photocatalytic activities of the samples have progressive increase. Naturally, the S7 - 6h produces the most acetone (1356 ppm), being nearly 8 times more than S0 - 6h (174 ppm). Meanwhile, the g-C_3N_4 produces only 111 ppm acetone at the same conditions. At the same time, the photooxidation of gaseous IPA over S7- 6h without irradiation were also carried out, and little acetone was produced (Figure S3).

Based on the individual physical properties of the α-Bi_2O_3 samples referred above, the photocatalytic activity enhancement is mainly caused by the BET surface area incrase of the sample. However, the increase of the sample's BET surface area is only less than 3 times. Obviously, the increase of the BET surface area is not enough to explain the improvement of the photocatalytic activity (800%). Besides the increasement of the BET surface area, the decrease of the (120) facet is the unique change between the microrod- and nanorod-like α - Bi_2O_3 samples, according to our characterization on different samples. It is widely reported that the exposed crystal planes play a critical role in determining the photocatalytic activity and efficiency, such as $AgPO_4$[19] and TiO_2[20]. Therefore, we speculate that the enhancement of the photocatalytic activity is also related to the decrease of the (120) facet exposure. In another word, the (120) facet is probably not an active facet for the photocatalytic oxidation of IPA.

The formation mechanism of the nanorod-like α-Bi_2O_3 nanoparticles from microrod-like α-Bi_2O_3, induced by g-C_3N_4, was studied detailedly by the combination of the TG-DTA and XRD. The TG-DTA experiments were carried out in almost the same manner with the prepared process of S7 - 6h. According to the TGA spectra in Figure 5, about 70% weight (3.5 mg in 5 mg) lost in the process of the heat treatment, corresponding to the weight fraction of g-C_3N_4 in the mixtures. Generally, pure g-C_3N_4 is stable in air below 600°C, but according to the report, the stability of g-C_3N_4 will significantly decrease when there is a second phase, such as $DyVO_4$[21]. Based on our results, we think the existence of α-Bi_2O_3 have the same effect on the stability of g-C_3N_4. Therefore, this result further explains the g-C_3N_4 totally dissolved out in the heat treatment process, being accordance with the XRD (Figure 3) and FT-IR (Figure S1) spectra. The DTA spectrum in Fig. 5 combined with the XRD spectra in Figure 6, we found that there are three thermonegative peaks for the S7 g-C_3N_4/α-Bi_2O_3 mixtures, while there is only one thermonegative peak for the pure α-Bi_2O_3 sample. The same thermonegative peak at about the 42nd minute can be attributed to the phase transition of Bi_2O_3 from α-phase to β-phase (metastable phase). After that, the thermonegative peak in the range of the 50th minute to the 250th minute, for the S7 g-C_3N_4/α-Bi_2O_3 mixtures, is ascribed to the decomposition of the g-C_3N_4, due to the rapidly weight loss in this period. Before the phase transition peak, at about the 40th minute, there is an unknown thermonegative peak emerged in the DTA spectrum of S7 g-C_3N_4/α-Bi_2O_3 mixtures. Considering the time and temperature of its emergence, we calcinate the S7 g-C_3N_4/α-Bi_2O_3 mixtures at 450°C for 30 minutes, with the temperature increase speed of 10°C/min, to study the composites of the reaction products at this condition. The XRD spectrum in Figure 6 helps us to uncover the truth, and tells us that the new component is finally determined to be the $Bi_2O_2CO_3$ crystals. Accordingly, the whole formation mechanism of the nanorod-like α-Bi_2O_3 nanoparticles from the microrod-like α-Bi_2O_3, induced by g-C_3N_4, can be described as follows: The g-C_3N_4 dissolves into CO_2 slowly at about 400°C; the released CO_2 corrodes the surfaces of the microrod-like α-Bi_2O_3 by reacting with the α-Bi_2O_3, producing the $Bi_2O_2CO_3$ crystals[22]; the $Bi_2O_2CO_3$ products further decompose into α-Bi_2O_3 and CO_2 again at 450°C[23, 24], resulting in the great changes of the microstructure for α-Bi_2O_3 (Scheme 1). In order to further confirm this conclusion, we also use the $(NH_4)_2CO_3$

(inorganics) and citric acid (organics) as the template to treat the microrod-like α-Bi_2O_3, and get the α-Bi_2O_3 samples with the similar microstructures [Figure S4 (A) and (B)].

By summary, the nanorod-like α-Bi_2O_3 nanoparticles were successfully transformed from the microrod-like α-Bi_2O_3, by using g-C_3N_4 as a template. The significant microstructure changes occurred in this process, resulting in the progressively decreases of particles and gradually increases of the surface areas. Besides, the formation mechanism of the nanorod-like α-Bi_2O_3 nanoparticles was further studied detailedly, and demonstrated to be the CO_2 corrosion effects. This work shows that the photocatalytic activity of α-Bi_2O_3 can be efficiently improved by decreasing its particle size, and promotes the research of α-Bi_2O_3 in the field of photocatalysis into a new step.

ACKNOWLEDGMENT

This work is supported by the National Natural Science Foundation of China (21273281), National Basic Research Program of China (973Program, No. 2013CB632405), the Fundamental Research Funds for the Central Universities and the Research Funds of Renmin University of China (13XNH121), and the China Scholarship Council.

Notes and references

[a] *Research Unit for Environmental Remediation Materials, National Institute for Materials Science (NIMS), 1-1, Namiki, Tsukuba, Ibaraki 305-0044, Japan, Email: Jinhua.YE@nims.go.jp*

[b] *Department of Chemistry, Renmin University of China, Beijing 100872, People's Republic of China*

†Electronic Supplementary Information (ESI) available: Sample characterizations, photocatalytic activity measurements, FT-IR spectrum, UV-vis DRS spectrum, the Photooxidation of IPA spectrum by S7 - 6h with and without irradiation, SEM of the α-Bi_2O_3 samples induced by $(NH_4)_2CO_3$ and citric acid.

1. X. Chen and S. S. Mao, *Chem. Rev.*, 2007, **107**, 2891-2959.
2. H. Tong, S. Ouyang, Y. Bi, N. Umezawa, M. Oshikiri and J. Ye, *Adv. Mater.*, 2012, **24**, 229-251.
3. G. Xi, Y. Yan, Q. Ma, J. Li, H. Yang, X. Lu and C. Wang, *Chem. Eur. J.*, 2012, **18**, 13949-13953.
4. M. Ge, Y. Li, L. Liu, Z. Zhou and W. Chen, *J. Phys. Chem. C*, 2011, **115**, 5220-5225.
5. H.-Y. Jiang, J. Liu, K. Cheng, W. Sun and J. Lin, *J. Phys. Chem. C*, 2013, **117**, 20029-20036.
6. H.-Y. Jiang, K. Cheng and J. Lin, *Phys. Chem. Chem. Phys.*, 2012, **14**, 12114-12121.
7. J. Eberl and H. Kisch, *Photochem. Photobiol. Sci.*, 2008, **7**, 1400-1406.
8. T. Saison, N. Chemin, C. Chanéac, O. Durupthy, V. Ruaux, L. Mariey, F. o. Maugé, P. Beaunier and J.-P. Jolivet, *J. Phys. Chem. C*, 2011, **115**, 5657-5666.
9. L. Zhou, W. Wang, H. Xu, S. Sun and M. Shang, *Chem. Eur. J.*, 2009, **15**, 1776-1782.
10. F. Qin, G. Li, R. Wang, J. Wu, H. Sun and R. Chen, *Chem. Eur. J.*, 2012, **18**, 16491-16497.
11. A. Hameed, T. Montini, V. Gombac and P. Fornasiero, *J. Am. Chem. Soc.*, 2008, **130**, 9658-9659.
12. S. Chen, Y. Hu, L. Ji, X. Jiang and X. Fu, *Appl. Sur. Sci.*, 2014, **292**, 357-366.
13. F. Qin, H. Zhao, G. Li, H. Yang, J. Li, R. Wang, Y. Liu, J. Hu, H. Sun and R. Chen, *Nanoscale*, 2014, **6**, 5402-5409.
14. G. Lin, D. Tan, F. Luo, D. Chen, Q. Zhao, J. Qiu and Z. Xu, *J. Alloys Compd.*, 2010, **507**, L43-L46.
15. X. Wang, K. Maeda, A. Thomas, K. Takanabe, G. Xin, J. M. Carlsson, K. Domen and M. Antonietti, *Nat. Mater.*, 2008, **8**, 76-80.
16. L. Huang, H. Xu, Y. Li, H. Li, X. Cheng, J. Xia, Y. Xu and G. Cai, *Dalton Trans.*, 2013, **42**, 8606-8616.
17. L. Ge, F. Zuo, J. Liu, Q. Ma, C. Wang, D. Sun, L. Bartels and P. Feng, *J. Phys. Chem. C*, 2012, **116**, 13708-13714.

18. B. Chai, T. Peng, J. Mao, K. Li and L. Zan, *Phys. Chem. Chem. Phys.*, 2012, **14**, 16745-16752.

19. Y. Bi, S. Ouyang, N. Umezawa, J. Cao and J. Ye, *J. Am. Chem. Soc.*, 2011, **133**, 6490-6492.

20. H. Xu, P. Reunchan, S. Ouyang, H. Tong, N. Umezawa, T. Kako and J. Ye, *Chem. Mater.*, 2013, **25**, 405-411.

21. Y. He, J. Cai, T. Li, Y. Wu, Y. Yi, M. Luo and L. Zhao, *Ind. Eng. Chem. Res.*, 2012, **51**, 14729-14737.

22. L. Huang, G. Li, T. Yan, J. Zheng and L. Li, *New J. Chem.*, 2011, **35**, 197-203.

23. G. Zhu, J. Lian, M. Hojamberdiev and W. Que, *J. Cluster Sci.*, 2013, **24**, 829-841.

24. Z. Ai, Y. Huang, S. Lee and L. Zhang, *J. Alloys Compd.*, 2011, **509**, 2044-2049.

Figure 1. SEM spectra of the α-Bi_2O_3 samples induced by g-C_3N_4 with the calcinations time of 3 and 6 hours

Figure 2. TEM image of the worm-like α-Bi_2O_3 nanoparticles (S7-6h)

Figure 3. XRD spectra of all the α-Bi_2O_3 samples induced by g-C_3N_4 with 6 hours' calcination

Figure 4. Acetone production over all the α-Bi_2O_3 samples induced by g-C_3N_4 with 6 hours' calcination

Figure 5. The TG-DTA spectra of the S7 g-C_3N_4/α-Bi_2O_3 mixtures

Figure 6. XRD spectra of the S7 g-C_3N_4/α-Bi_2O_3 mixtures after the calcination at 450°C for 30 minutes

Scheme 1. The formation mechanism of worm-like α-Bi_2O_3 from microrod-like α-Bi_2O_3

Table 1. **BET Surface Areas of the α - Bi_2O_3 with Different microstructures**

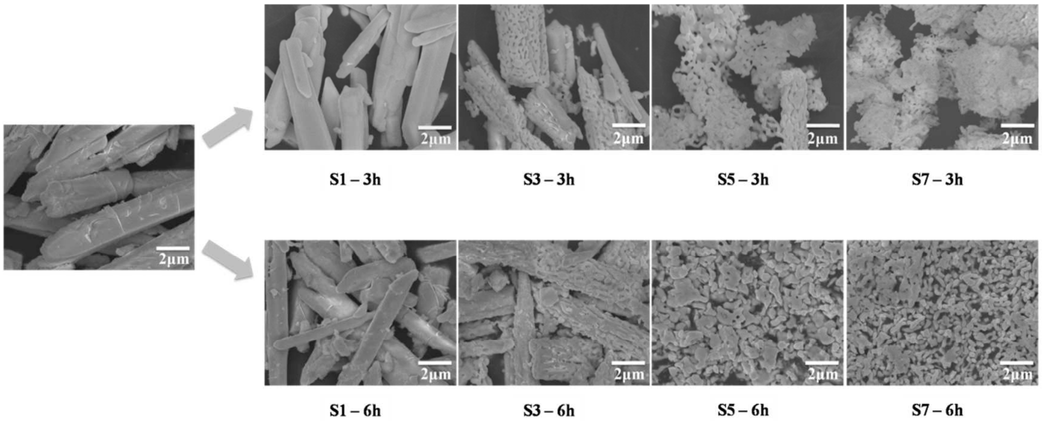
2µm
2µm
2µm
2µm
2µm
S1 – 3h
S3 – 3h
S5 – 3h
S7 – 3h
2µm
2µm
2µm
2µm
S1 – 6h
S3 – 6h
S5 – 6h
S7 – 6h

Fig. 1

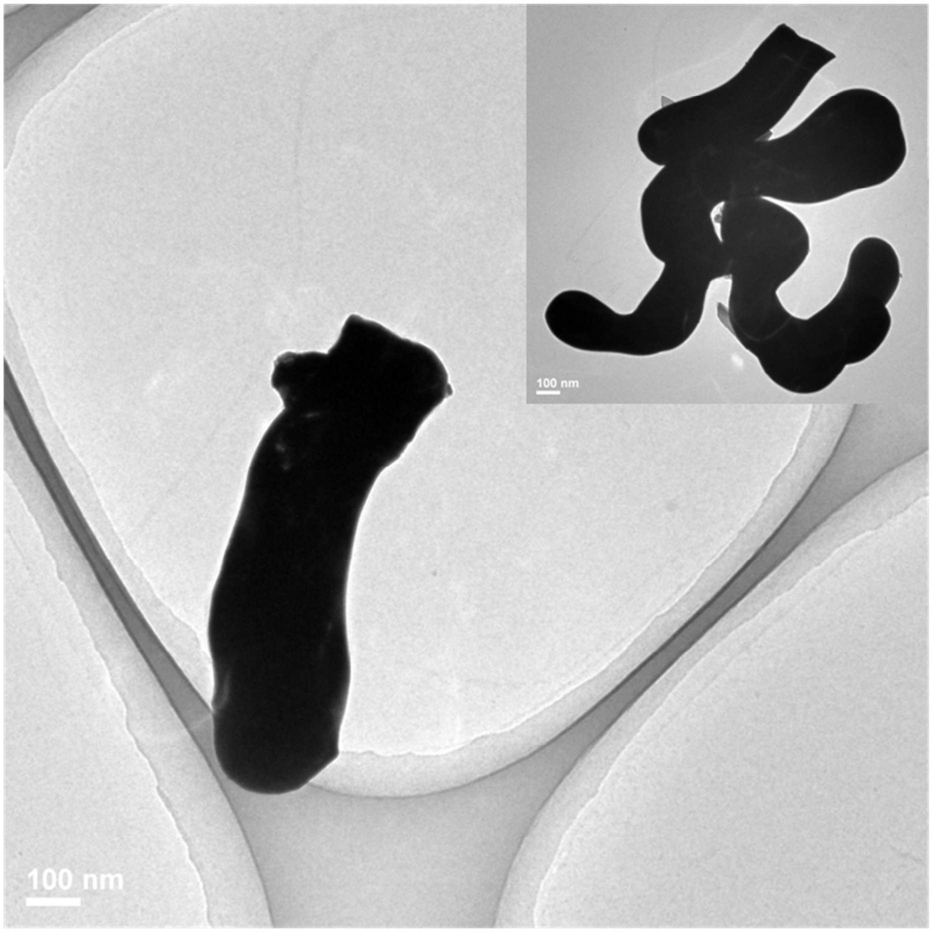
100 nm
100 nm

Fig. 2

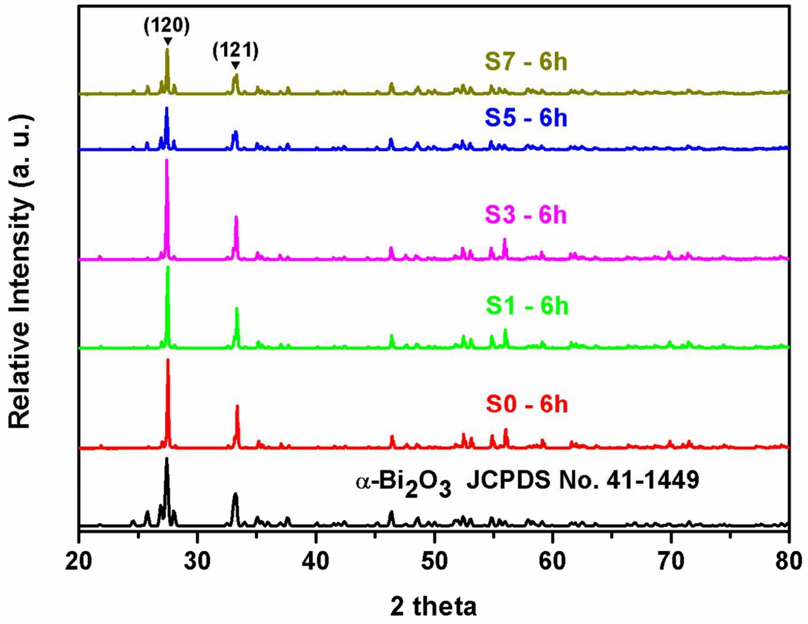

Fig. 3

$$CH_3CH(OH)CH_3 \xrightarrow[\textit{Photocatalyst}]{h\nu\ (\lambda \geq 420\text{nm})} CH_3COCH_3$$

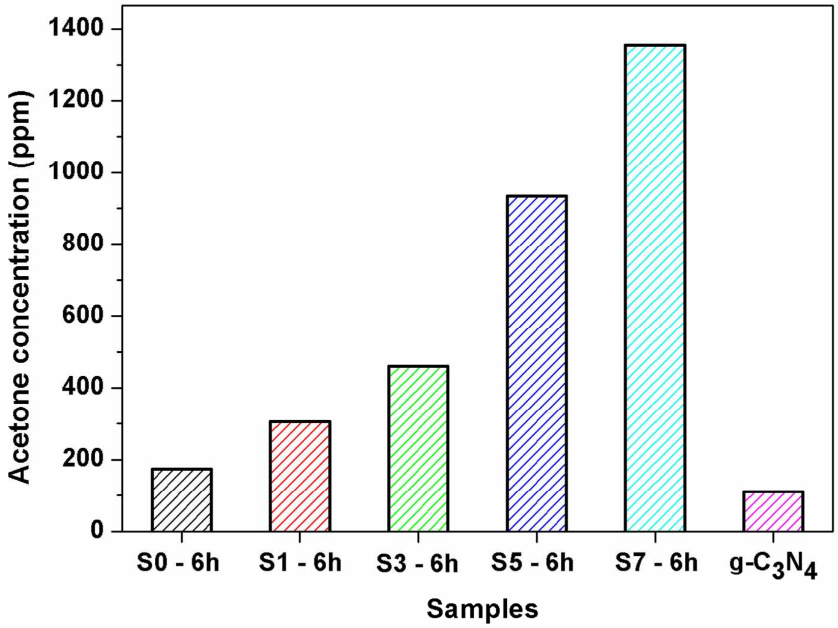

Fig. 4

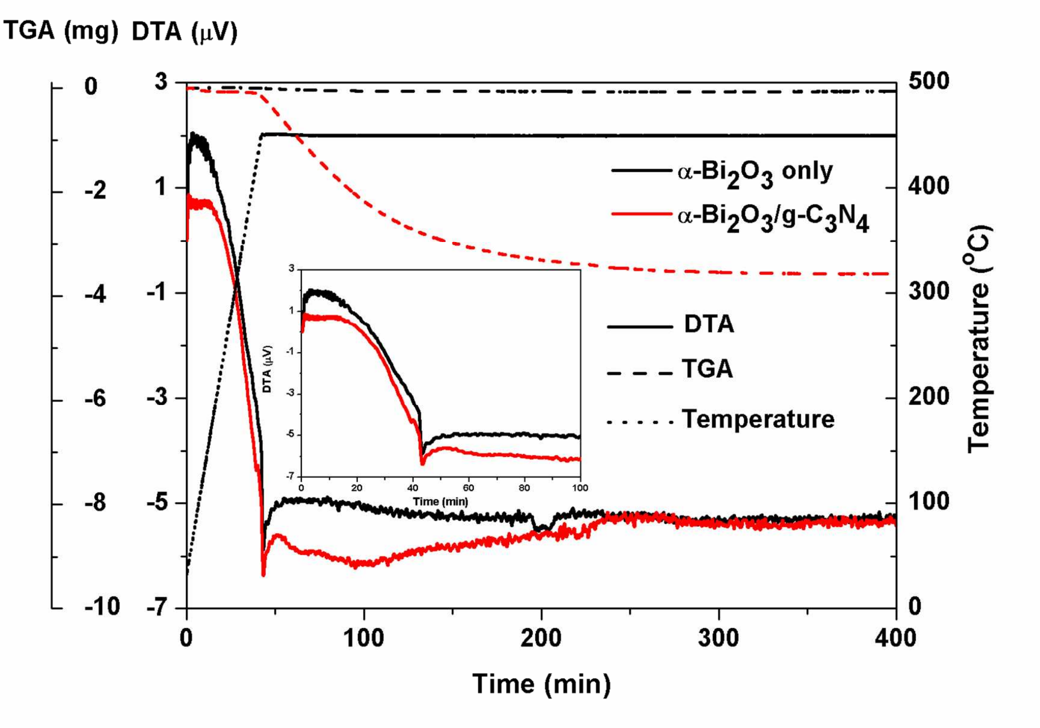
TGA (mg)
DTA (μV)
Temperature (°C)
Time (min)
α-Bi_2O_3 only
α-Bi_2O_3/g-C_3N_4
DTA
TGA
Temperature
0
-2
-4
-6
-8
-10
3
1
-1
-3
-5
-7
500
400
300
200
100
0
0
100
200
300
400
DTA (μV)
Time (min)

Fig. 5

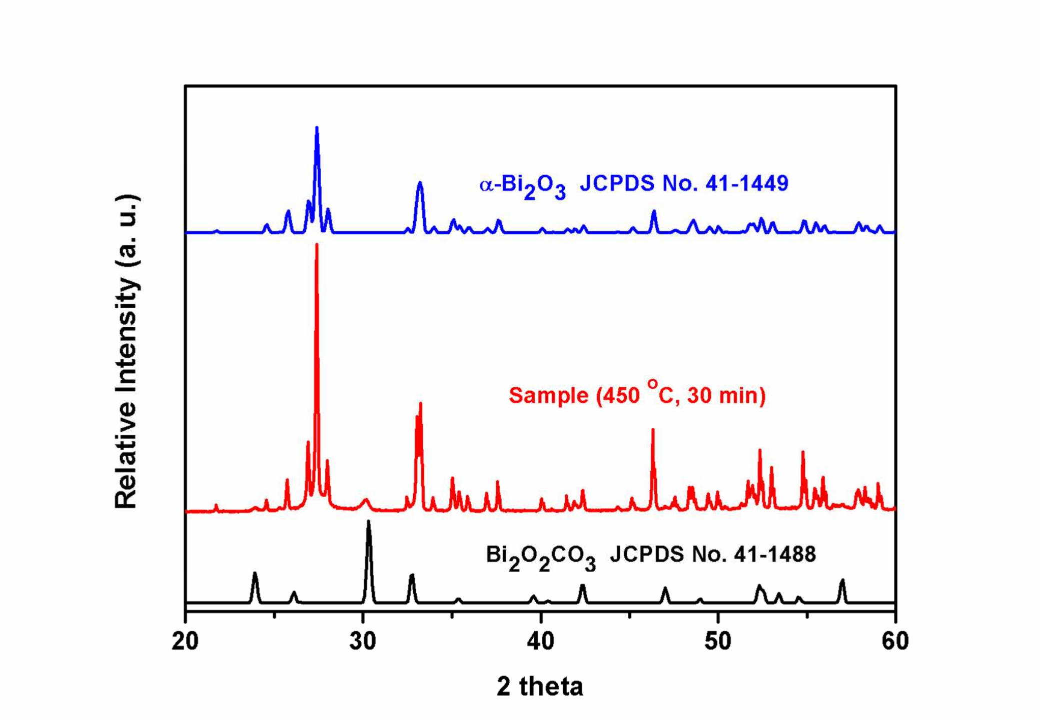
Relative Intensity (a. u.)
α-Bi_2O_3 JCPDS No. 41-1449
Sample (450 °C, 30 min)
$Bi_2O_2CO_3$ JCPDS No. 41-1488
20
30
40
50
60
2 theta

Fig. 6

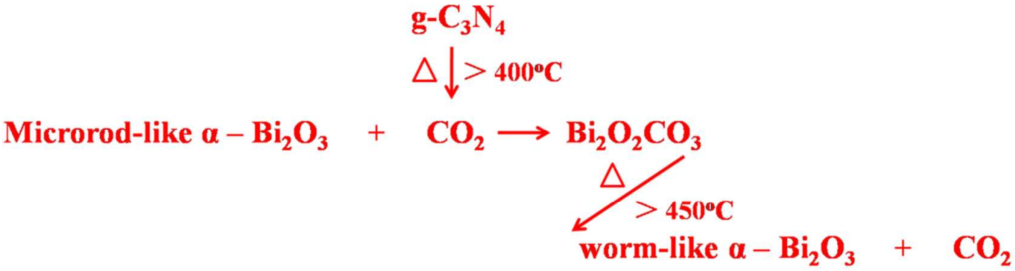

Scheme 1

Samples	S0 - 6h	S1 – 6h	S3 – 6h	S5 – 6h	S7 – 6h
BET surf. Area (m^2/g)	0.80 ± 0.10	0.80 ± 0.10	1.0 ± 0.10	1.2 ± 0.10	2.4 ± 0.10

Table 1

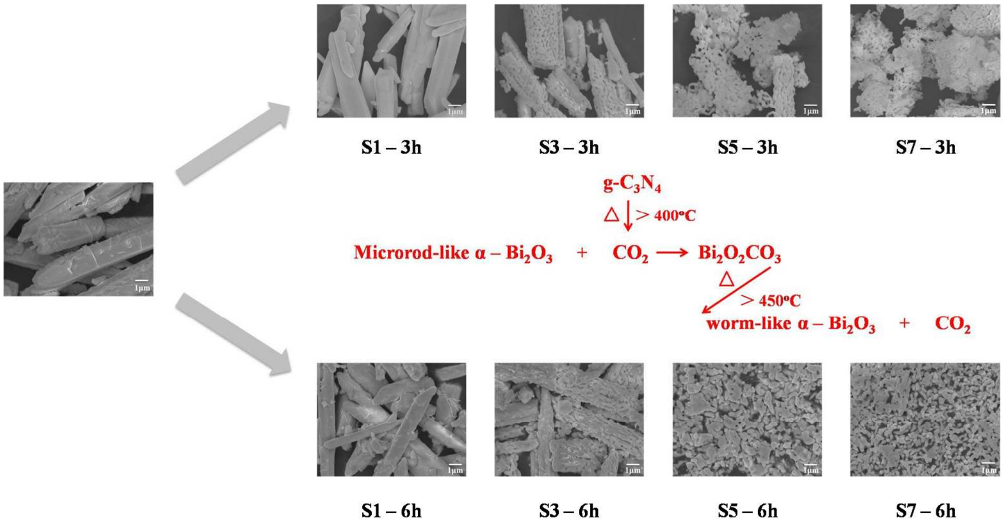

323x168mm (150 x 150 DPI)